Crystal Structures of the Wild-Type, P1A Mutant, and Inactivated Malonate Semialdehyde Decarboxylase: A Structural Basis for the Decarboxylase and Hydratase Activities[†,‡]

Jeffrey J. Almrud,[§,||] Gerrit J. Poelarends,[§,||,⊥] William H. Johnson, Jr.,[§] Hector Serrano,[§] Marvin L. Hackert,[@] and Christian P. Whitman*[,§]

Division of Medicinal Chemistry, College of Pharmacy, and Department of Chemistry and Biochemistry, The University of Texas, Austin, Texas 78712-1074

Received July 15, 2005; Revised Manuscript Received September 12, 2005

ABSTRACT: Malonate semialdehyde decarboxylase (MSAD) from *Pseudomonas pavonaceae* 170 is a tautomerase superfamily member that converts malonate semialdehyde to acetaldehyde by a mechanism utilizing Pro-1 and Arg-75. Pro-1 and Arg-75 have also been implicated in the hydratase activity of MSAD in which 2-oxo-3-pentynoate is processed to acetopyruvate. Crystal structures of MSAD (1.8 Å resolution), the P1A mutant of MSAD (2.7 Å resolution), and MSAD inactivated by 3-chloropropiolate (1.6 Å resolution), a mechanism-based inhibitor activated by the hydratase activity of MSAD, have been determined. A comparison of the P1A-MSAD and MSAD structures reveals little geometric alteration, indicating that Pro-1 plays an important catalytic role but not a critical structural role. The structures of wild-type MSAD and MSAD covalently modified at Pro-1 by 3-oxopropanoate, the adduct resulting from the incubation of MSAD and 3-chloropropiolate, implicate Asp-37 as the residue that activates a water molecule for attack at C-3 of 3-chloropropiolate to initiate a Michael addition of water. The interactions of Arg-73 and Arg-75 with the C-1 carboxylate group of the adduct suggest these residues polarize the α,β-unsaturated acid and facilitate the addition of water. On the basis of these structures, a mechanism for the inactivation of MSAD by 3-chloropropiolate can be formulated along with mechanisms for the decarboxylase and hydratase activities. The results also provide additional evidence supporting the hypothesis that MSAD and *trans*-3-chloroacrylic acid dehalogenase, a tautomerase superfamily member preceding MSAD in the *trans*-1,3-dichloropropene degradation pathway, diverged from a common ancestor but retained the key elements for the conjugate addition of water.

Mechanisms for the enzymatic and nonenzymatic decarboxylation of β-keto acids have been extensively studied (*1*−*7*). The three major mechanisms observed in the enzyme-catalyzed reactions involve Schiff base catalysis (*3*, *4*), a metal ion cofactor (*5*, *6*), or hydrogen bonding interactions (*7*). These strategies facilitate decarboxylation by interacting with the ketone (or aldehyde) carbonyl group and providing an electron sink to stabilize the carbanion that forms upon loss of the carbon dioxide. Further rate acceleration can be obtained by two additional strategies. First, the departing carboxylate group can be positioned into a hydrophobic pocket to destabilize the negative charge. Second, the carboxylate group can be oriented so that the scissile bond is aligned parallel to the p-orbitals of the carbonyl group. In this conformation, decarboxylation is favorable (*8*).

Scheme 1

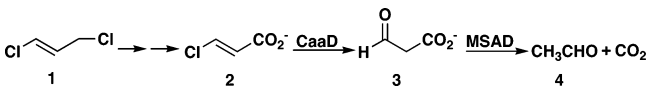

Malonate semialdehyde decarboxylase (MSAD),[1] a homotrimer in which each monomer consists of 129 amino acids, catalyzes the metal ion-independent decarboxylation of the β-keto acid analogue, malonate semialdehyde (**3**, Scheme 1), to afford acetaldehyde (**4**) and carbon dioxide (*9*). The enzyme is part of a pathway elaborated by *Pseudomonas pavonaceae* 170 and other soil bacteria for

[†] This research was supported by National Institutes of Health Grant GM-65324 (C.P.W. and M.L.H.) and the Robert A. Welch Foundation (Grants F-1334 and F-1219).

[‡] The coordinates have been deposited in the Protein Data Bank (PDB entries 2AAG, 2AAJ, and 2AAL).

* To whom correspondence should be addressed. Phone: (512) 471-6198. Fax: (512) 232-2606. E-mail: whitman@mail.utexas.edu.

[§] Division of Medicinal Chemistry.

[||] These authors contributed equally to this work.

[⊥] Present address: Department of Biochemistry, Groningen Biomolecular Sciences and Biotechnology Institute, University of Groningen, Nijenborgh 4, 9747 AG Groningen, The Netherlands.

[@] Department of Chemistry and Biochemistry.

[1] Abbreviations: CHMI, 5-carboxymethyl-2-hydroxymuconate isomerase; CaaD, *trans*-3-chloroacrylic acid dehalogenase; *cis*-CaaD, *cis*-3-chloroacrylic acid dehalogenase; *p*-CMPS, *p*-chloromercuriphenylsulfonate; ESI-MS, electrospray ionization mass spectrometry; F_o and F_c, observed and calculated structure factors, respectively; HPLC, high-pressure liquid chromatography; MALDI-PSD, matrix-assisted laser desorption ionization postsource decay; MALDI-TOF, matrix-assisted laser desorption ionization time-of-flight; MSAD, malonate semialdehyde decarboxylase; MIF, macrophage migration inhibitory factor; 4-OT, 4-oxalocrotonate tautomerase; PPT, phenylpyruvate tautomerase; rmsd, root-mean-square deviation; SDS−PAGE, sodium dodecyl sulfate−polyacrylamide gel electrophoresis.

10.1021/bi051383m CCC: $30.25
Published on Web 10/21/2005

Scheme 2

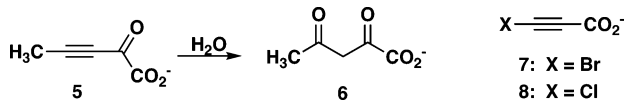

the degradation of the nematocide *trans*-1,3-dichloropropene (**1**) (*10*). In addition to this presumed physiological decarboxylase activity, MSAD exhibits a hydratase activity as demonstrated by its conversion of 2-oxo-3-pentynoate (**5**, Scheme 2) to acetopyruvate (**6**) (*11*). MSAD is classified as a member of the tautomerase superfamily, which is a group of structurally homologous proteins having a common $\beta-\alpha-\beta$ fold and a catalytic amino-terminal proline (*9*).

A combination of studies on MSAD implicated Pro-1, with a pK_a of ~9.2, and Arg-75 in the decarboxylation and hydration mechanisms (*9*, *11*, *12*). In the proposed decarboxylation mechanism, the cationic Pro-1 polarizes the C-3 carbonyl group of **3** by hydrogen bonding and/or an electrostatic interaction and Arg-75 positions the carboxylate group in a favorable orientation for decarboxylation. In the proposed hydration mechanism, a water molecule, activated by an unknown residue, adds to C-4 of **5** to initiate a Michael reaction. An interaction between the C-2 carbonyl group and Arg-75 may polarize the α,β-unsaturated bond and facilitate the addition of water to the triple bond. Protonation of the resulting allenic species at C-3 by Pro-1 would complete the reaction. The recently described irreversible inactivation of MSAD by 3-bromo- and 3-chloropropiolate (**7** and **8**, respectively, in Scheme 2) is a consequence of the hydratase activity (*12*).

To obtain further insight into the decarboxylation and hydration mechanisms, crystal structures were determined for the wild-type enzyme (to 1.8 Å resolution), the P1A mutant (to 2.7 Å resolution), and the enzyme inactivated by **8** (to 1.6 Å resolution). The three crystal structures confirm that MSAD is a trimer whose subunits are constructed from a gene duplication of the signature $\beta-\alpha-\beta$ building block. The wild-type structure validates the metal ion independence of the reaction because no metal ion is observed in the structure despite the presence of high concentrations of Mg^{2+} in the crystallization conditions. The structure of the inactivated enzyme clearly shows modification of Pro-1 by a 3-oxopropanoate moiety, consistent with an earlier mass spectral analysis (*12*). The positioning of the adduct implicates two additional active site residues, Asp-37 and Arg-73, in the decarboxylation and hydration mechanisms. Replacement of these residues with an asparagine (D37N) or an alanine (R73A) results in mutants with substantially reduced decarboxylase and hydratase activities. The combined results provide a more complete reaction mechanism for both activities and are consistent with the hypothesis that MSAD and *trans*-3-chloroacrylic acid dehalogenase (CaaD), the preceding enzyme in the *trans*-1,3-dichloropropene degradation pathway (*10*), diverged from a common ancestor, which might have carried out the conjugate addition of water to an α,β-unsaturated acid as well as the decarboxylation of a β-keto acid.

EXPERIMENTAL PROCEDURES

Materials. The sources for the components of Luria-Bertani (LB) medium as well as the enzymes and reagents used in the molecular biology procedures are reported elsewhere (*9*). The Amicon concentrator and the YM10 ultrafiltration membranes were obtained from Millipore Corp. (Bedford, MA). Prepacked PD-10 Sephadex G-25 columns were purchased from Biosciences AB (Uppsala, Sweden). Oligonucleotides for DNA amplification and sequencing were synthesized by Genosys (The Woodlands, TX). The synthesis of 3-chloropropiolate (**8**) is reported elsewhere (*13*).

Bacterial Strains, Plasmids, and Growth Conditions. *Escherichia coli* strain BL21-Gold(DE3) was obtained from Stratagene (La Jolla, CA), and was used for the cloning of the genes for the D37N and R73A mutants of MSAD, plasmid DNA isolation, and the overproduction of MSAD and the three mutants (P1A, D37N, and R73A) of MSAD. The construction of the plasmids for MSAD and the P1A mutant is described elsewhere (*9*). The pET3b expression vector (Stratagene) was used for the expression of the D37N and R73A mutant genes. The *E. coli* strains were grown at 30 °C in LB medium. When required, Difco agar (15 g/L) and ampicillin (100 μg/mL) were added to the medium.

General Enzymology Methods. General procedures for cloning and DNA manipulation were performed as described elsewhere (*14*). The PCR was carried out in a Perkin-Elmer model 480 DNA thermocycler obtained from Perkin Elmer Inc. (Wellesley, MA). DNA sequencing was performed by the DNA Core Facility in the Institute for Cellular and Molecular Biology at The University of Texas. HPLC was performed on a Waters (Milford, MA) 501/510 system using either a TSKgel DEAE-5PW (anion exchange) or a TSKgel Phenyl-5PW (hydrophobic interaction) column (Tosoh Bioscience, Montgomeryville, PA). MSAD and the mutants were purified to homogeneity, as assessed by sodium dodecyl sulfate−polyacrylamide gel electrophoresis (SDS−PAGE), according to a published procedure (*9*). Protein was analyzed by SDS−PAGE on gels containing 15% polyacrylamide (*15*). The gels were stained with Coomassie brilliant blue. Protein concentrations were determined by the method of Waddell (*16*). The native molecular masses of the D37N and R73A mutants were determined by gel filtration on a Superose 12 column (Pharmacia Biotech AB, Uppsala, Sweden) using the Waters 501/510 HPLC system. Absorbance data were obtained on a Hewlett-Packard 8452A diode array spectrophotometer.

Construction of the D37N and R73A Mutants of MSAD. The D37N and R73A mutants were generated by overlap extension PCR (*17*) using plasmid pET(orf130) as the template (*9*). For the D37N and R73A mutants, the oligonucleotides, 5′-ATA**CATATG**CCACTTCTCAAGTTC-3′ and 5′-CAT**GGATCC**TCAGACGAGGTCCCCAGT-3′, were used as the forward and reverse external primers, respectively. The forward primer contains a *Nde*I restriction site (in bold), and the reverse primer has a *Bam*HI restriction site (in bold). For the D37N mutant, the internal PCR primers were oligonucleotides 5′-GTCCCTGCAAATAATCGCTAC-CAAACAGTA-3′ and 5′-TACTGTTTGGTAGCGATTATT-TGCAGGGAC-3′. For the R73A mutant, the internal PCR primers were oligonucleotides 5′-ACCGTGATATCTGCAC-CTCGATCA-3′ and 5′-TGATCGAGGTGCAGATATCACG-GT-3′. The codons for introducing the mutations are underlined. The amplification mixtures contained the appropriate synthetic primers, the deoxynucleotide triphosphates, template DNA (~100 μg), and the PCR reagents

supplied in the Expand High Fidelity PCR system (D37N) or those in the Taq DNA polymerase system (R73A) (F. Hoffmann-LaRoche, Ltd., Basel, Switzerland). Restriction sites *Nde*I and *Bam*HI, introduced during the amplification reaction, were used to clone the purified PCR products into plasmid pET3b for overexpression of the mutants. The cloned genes were sequenced to verify that only the desired mutation had been introduced during the PCR.

Mass Spectrometric Characterization of the MSAD Mutants. The masses of the D37N and R73A mutants were determined using an LCQ electrospray ion trap mass spectrometer (ThermoFinnigan, San Jose, CA), housed in the Analytical Instrumentation Facility Core in the College of Pharmacy at The University of Texas. The protein samples were made up as described elsewhere (*18*). The observed monomer masses were 14 105 Da (calcd 14 105 Da) for the D37N mutant and 14 022 Da (calcd 14 024 Da) for the R73A mutant.

Enzyme Assays. MSAD activity was monitored by following the decrease in NADH absorbance at 340 nm in a coupled assay using the β-NADH-dependent alcohol dehydrogenase at 22 °C as described previously (*9*). The hydration of 2-oxo-3-pentynoate (**5**) was monitored by following the formation of acetopyruvate (**6**) at 294 nm and 22 °C as described elsewhere (*18*).

*Inactivation of MSAD by 3-Chloropropiolate (**8**)*. MSAD was inactivated by 3-chloropropiolate (**8**) using a published protocol with the following modifications (*12*). The enzyme (1.35 mM based on the molecular mass of the monomer) was incubated with an excess (~7:1) of **8** (10 mM) in 1.2 mL of 10 mM Tris-SO_4 buffer (pH 7.0) for 24 h at 4 °C. Subsequently, the sample was loaded onto a PD-10 Sephadex G-25 gel filtration column, which had previously been equilibrated with 10 mM Tris-SO_4 buffer (pH 7.0). The protein was eluted with the same buffer by gravity flow. Fractions (0.5 mL) were analyzed for the presence of protein by UV absorbance at 214 nm. The purified enzyme was concentrated to ~20 mg/mL and assayed for residual hydratase activity as described above. The protein sample treated with **8** had no detectable activity.

*Crystallization and Structure Determination of MSAD, the P1A Mutant, and MSAD Inactivated by **8***. The crystallization conditions and the experimental procedures used for data collection and the structure determination of MSAD, the P1A mutant, and MSAD inactivated by **8** are provided in the Supporting Information. The heavy atom derivative screening and the subsequent structure determination of the MSAD−*p*-chloromercuriphenylsulfonate (*p*-CMPS) complex are also provided in the Supporting Information. A summary of the data collection statistics for four structures (MSAD, the MSAD−*p*-CMPS complex, the P1A mutant of MSAD, and MSAD inactivated by **8**) is provided in Table 1, and a summary of the refinement statistics for three structures (MSAD, the P1A mutant of MSAD, and MSAD inactivated by **8**) is provided in Table 2.

Table 1: Data Collection Statistics

	MSAD	MSAD−*p*-CMPS	P1A mutant	MSAD inactivated by **8**
space group	$P2_1$	$P6_3$	$P2_13$	$P3_2$
resolution (Å)	30.0−1.8	30.0−2.1	30.0−2.7	72.6−1.6
no. of independent reflections	60986	78294	11976	86122
completeness (%)	96.4	88.0	99.4	98.8
$\langle I/\sigma(I)\rangle$	12.2	21.9	5.3	3.5
R_{sym} (%)	7.2	7.2	12.9	12.7
figure of merit	0.72			

Table 2: Structure Refinement Statistics for MSAD, the P1A Mutant, and MSAD Inactivated by **8**

	MSAD	P1A mutant	MSAD inactivated by **8**
resolution limits (Å)	19.2−1.8	29.4−2.7	72.6−1.6
R factor (%)	18.4	15.8	18.4
R_{free} (%)	23.3	21.2	23.8
no. of reflections used	55695	11251	74759
no. of protein atoms	5963	1973	6170
no. of water atoms	826	243	958
protein *B*-factor	22.3	32.1	10.1
water *B*-factor	34.1	38.6	21.6
weighted root-mean-square deviation from ideality			
bond lengths (Å)	0.03	0.02	0.03
bond angles (deg)	2.3	2.04	2.5
torsion angles (deg)	8.0	7.71	8.30
Ramachandran plot			
residues in the core region (%)	90.6	92.8	90.0
residues in the allowed region (%)	9.4	7.2	10.0
residues in the generous region (%)	0.0	0.0	0.0
residues in the disallowed region (%)	0.0	0.0	0.0

RESULTS AND DISCUSSION

Structure of Wild-Type MSAD. The wild-type MSAD crystal structure was determined to 1.8 Å resolution using heavy-atom methods, and refined to *R* and R_{free} values of 18.4 and 23.3%, respectively. The crystal structure confirms that MSAD is a homotrimer, and shows that the cylindrical molecule has overall dimensions of approximately 55 Å in diameter and 40 Å in height (Figure 1A). Crystals of wild-type MSAD grown in 1,6-hexanediol have two trimers per asymmetric unit. Both trimers are nearly identical with respect to one another, having a root-mean-square deviation (rmsd) of 0.13 Å^2 calculated for all backbone atoms and a value of 0.29 Å^2 calculated for all main chain and side chain atoms. The MSAD monomer consists of 129 amino acid residues whose secondary structure is composed of six β-strands (β-1−β-6), two α-helices, a 3_{10}-helix, and isolated β-bridges (Figure 1B). The protein fold is defined by β-1 (residues 1−8) near the amino terminus followed by α-1 (residues 13−31), β-2 (residues 39−45), β-3 (residues 50−52), β-4 (residues 66−72), α-2 (residues 77−95), a 3_{10}-helix (residues 99−101), β-5 (residues 102−108), and β-6 (residues 114−117) near the carboxyl terminus. β-Strands β-5, β-4, β-1, and β-2 coalesce to form a β-sheet where the two central strands run antiparallel relative to one another, and the two outer strands are parallel to their adjacent inner strands. The monomer's two α-helices are spatially positioned exterior to the β-sheet, and run antiparallel with respect to one another. MSAD has three active sites that are equivalently positioned at the same end of the trimer and are related to one another by a 120° rotation about the molecular 3-fold axis. Stabilization of the homotrimer is due, in part, to the extension of the four-stranded β-sheet to a six-stranded sheet composed of strands from all three

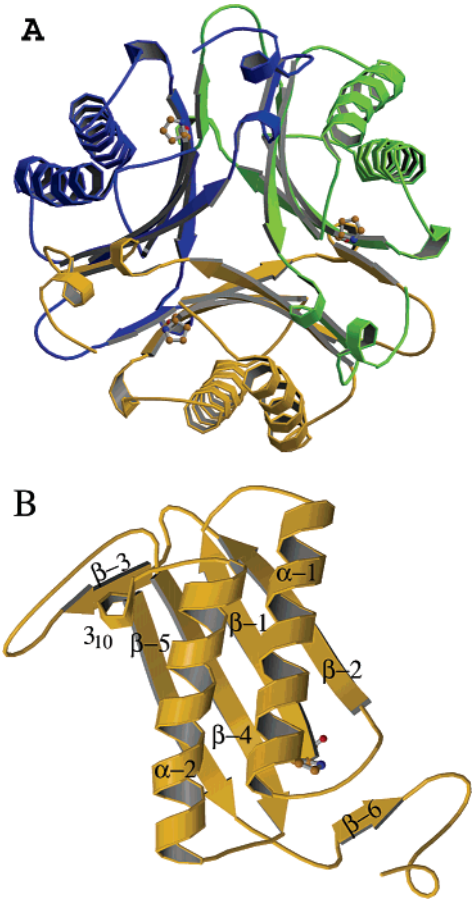

FIGURE 1: Ribbon diagrams representing the three-dimensional structures of the MSAD homotrimer and monomer. (A) MSAD homotrimer in which the individual monomers are colored blue, green, and gold. Pro-1 is shown for each monomer. (B) MSAD monomer, illustrating the signature $\beta-\alpha-\beta$ structural fold of known tautomerase superfamily members, with a ball-and-stick representation of the catalytic Pro-1. Secondary structural elements are labeled accordingly. This figure was prepared using MOLSCRIPT (*19*) and RASTER3D (*20*).

monomeric units as follows: $\uparrow\beta6'-\downarrow\beta5-\downarrow\beta4-\uparrow\beta1-\uparrow\beta2-\downarrow\beta3''$.[2]

Active Site of MSAD. The presence of an amino-terminal proline at the bottom of three clefts on the protein implicates these regions as the active sites. The MSAD active sites are approximately 10 Å × 6 Å × 10 Å in size. As with other tautomerase superfamily members (*21*−*24*), the active site of MSAD has a relatively simple architecture. With the exception of Thr-55′ from a neighboring monomer (designated by a prime), the MSAD active site consists of residues from a single monomer. One face of the active site is formed by the side chains of residues Arg-73, Arg-75, Val-33, and Asp-37 (Figures 2 and 3). The floor of the active site is formed by Pro-1, Leu-2, Trp-114, and Ser-72, and the back wall of the active site is formed by residues Tyr-39, Thr-55′, Phe-116, Phe-123, and Leu-128. The active site can also be divided into a hydrophobic region consisting of Trp-114, Phe-116, Phe-123, and Leu-128 and a hydrophilic region consisting of Pro-1, Asp-37, Ser-72, and two arginine residues (Arg-73 and Arg-75).

[2] The unprimed, primed, and doubly primed β-strands indicate that these β-strands come from different subunits of the MSAD trimer.

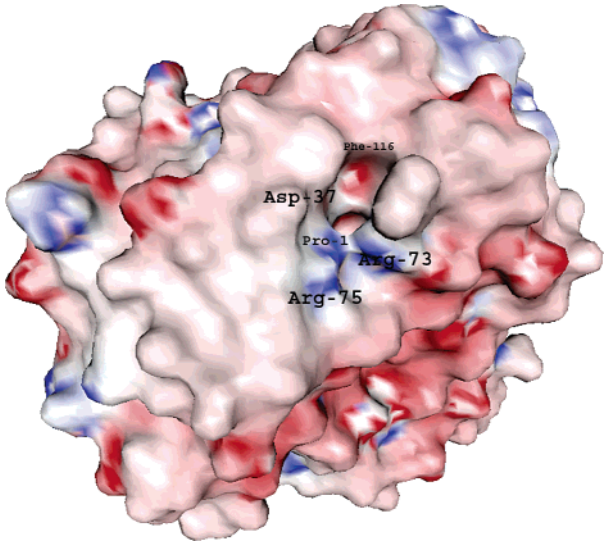

FIGURE 2: Electrostatic surface potential of the MSAD trimer showing an active site cavity. Active site residues Pro-1, Asp-37, Arg-73, Arg-75, and Phe-116 are labeled. Electropositive regions are depicted in shades of blue and the electronegative regions in shades of red. This figure was prepared using GRASS (*25*).

The MSAD active site has a network of ordered water molecules (Figure 3). One water molecule is within hydrogen bonding distance of the Pro-1 nitrogen (2.8 Å). Ordered water molecules are also observed within hydrogen bonding distance of the side chain hydroxyl oxygen of Thr-55′ (2.7 Å), the backbone nitrogen of Arg-73 (3.2 Å), and one of the η-nitrogens of Arg-75 (3.0 Å). In addition, one of the two η-nitrogens of the side chain guanidinium group of Arg-73 is within hydrogen bonding distance of a water molecule (3.0 Å), while the second η-nitrogen interacts with Asp-111 (2.9 Å) of the same monomer. Finally, there is an ordered water molecule within hydrogen bonding distance of a carboxylate oxygen of Asp-37 (2.6 Å).

Three additional observations provide structural validations for previous experimental results. First, there are no metal ions in the active site, although the enzyme was crystallized in the presence of 200 mM $MgCl_2$. This observation is consistent with the results of two earlier experiments, showing that neither incubation of the enzyme with EDTA nor the addition of metal ions affects decarboxylase activity (*9*). Second, Arg-75, identified by sequence analysis and site-directed mutagenesis as a potential active site residue, is indeed found in the active site. This observation is consistent with the fact that mutation of Arg-75 to an alanine results in a mutant with 0.17% of wild-type decarboxylase specific activity and no detectable hydratase activity (*9*, *11*). Finally, as expected, Arg-11 is not in the active site, but is located on a loop approximately 10 Å from the active site. This observation is consistent with the fact that replacing Arg-11 with an alanine had a negligible effect on the decarboxylase activity (*9*).

Comparison of MSAD with Tautomerase Superfamily Members. The tautomerase superfamily consists of five known families represented by their title enzymes, 5-carboxymethyl-2-hydroxymuconate isomerase (CHMI), 4-OT, macrophage migration inhibitory factor (MIF), *cis*-CaaD, and MSAD (*9*, *23*, *27*−*29*). CaaD is a member of a subfamily of the 4-OT family (*23*). CHMI, from *E. coli C* (*30*), and 4-OT, from *Pseudomonas putida* mt-2 (*31*), function as

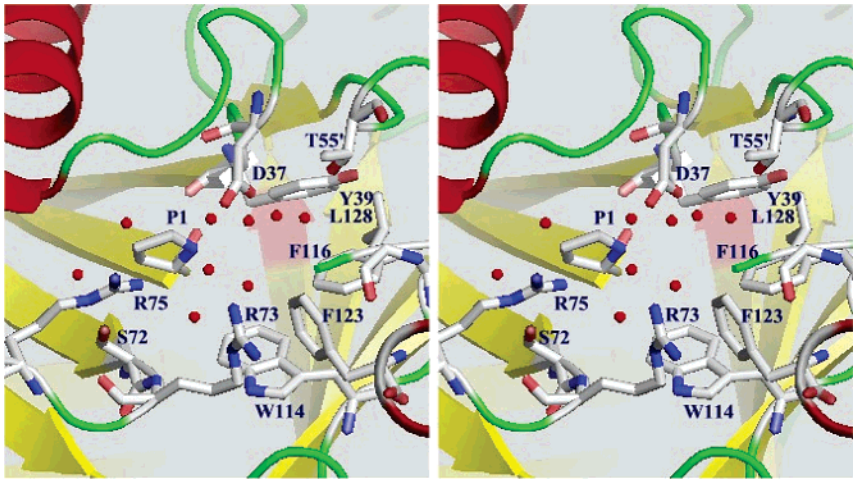

FIGURE 3: Stereodiagram of the active site of wild-type MSAD illustrating the hydrophobic (Trp-114, Phe-116, Phe-123, and Leu-128) and hydrophilic (Pro-1, Asp-37, Ser-72, Arg-73, and Arg-75) nature of the cavity. The active site is also filled with a network of hydrogen-bonded water molecules (colored red). This figure was prepared with PyMOL (*26*).

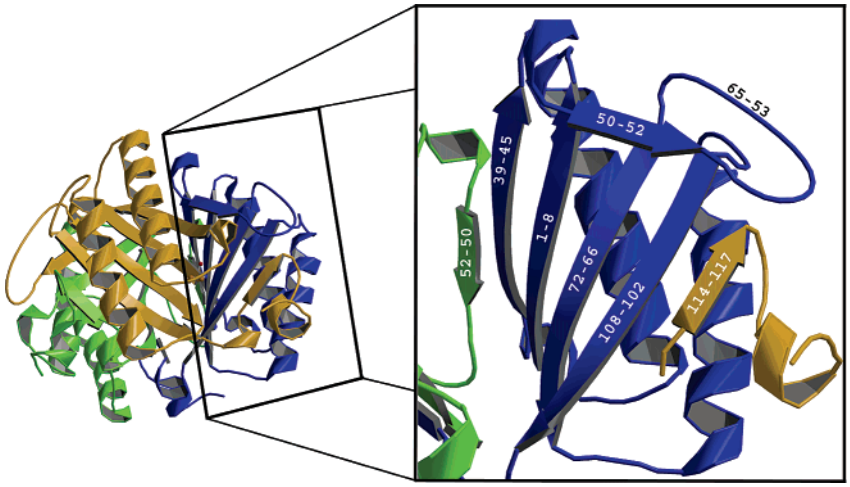

FIGURE 4: Ribbon diagram highlighting the structural elements responsible for stabilizing the MSAD trimer. The left panel shows the trimer in Figure 1A rotated ~70° toward the viewer. The individual monomers are represented by different colors. The right panel shows the interactions among the three monomers. The central core of the β-sheet of one monomer (blue) is extended by residues 114−117 (β-6′) from a second monomer (gold) and residues 50−52 (β-3″) from a third monomer (green) to stabilize the trimer. This figure was prepared with MOLSCRIPT (*19*) and Adobe Photoshop 7.0.

tautomerases in degradation pathways for aromatic amino acids (CHMI) and aromatic hydrocarbons (4-OT). MIF is a mammalian cytokine with a phenylpyruvate tautomerase (PPT) activity (*32*). CaaD and *cis*-CaaD precede MSAD in the degradation pathway for the nematocide, 1,3-dichloropropene (**1**, Scheme 1) (*10*).

Least-squares superpositioning of the C_α atoms of wild-type MSAD with CHMI (PDB entry 1OTG), 4-OT (PDB entry 4OTB), MIF (PDB entry 1MIF), and CaaD inactivated by **8** (PDB entry 1S0Y) revealed that the MSAD homotrimer is structurally most similar to the CaaD heterohexamer inactivated by **8** (3.9 Å rmsd), followed by the 4-OT homohexamer (4.6 Å rmsd), the CHMI homotrimer (8.3 Å rmsd), and the MIF homotrimer (13.1 Å rmsd).[3] The large disparity in the superpositioning of CHMI or MIF with MSAD is reduced when loops are eliminated from the calculations. However, appreciable differences in the tilts and twists in the α-helices and β-sheets remain.

[3] Coordinates for wild-type CaaD and *cis*-CaaD are not yet available.

Unlike CaaD, 4-OT, and the structurally homologous family member, YwhB from *Bacillus subtilis* (*28*), MSAD does not have a β-hairpin to stabilize its quaternary structure. Instead, the central core of the β-sheet of one monomer is extended by residues 114−117 (β-6′) from a second monomer and residues 50−52 (β-3″) from a third monomer to stabilize the trimer (Figure 4). The β-3″ strand is part of a large insert composed of residues 45−65. These residues also distinguish the MSAD trimer from those of MIF and CHMI. In MIF and CHMI, the secondary structures corresponding to the loop formed by residues 53−65 in MSAD are short loops. The loop in MIF is formed by residues 51−56, whereas the loop in CHMI is formed by residues 53−59. The additional residues in the MSAD loop result in more flexibility, and flip the loop approximately 90° relative to the corresponding loops in MIF and CHMI.

Crystal Structure of the P1A Mutant of MSAD. Replacing Pro-1 with an alanine significantly diminishes the decarboxylase activity (~1.4% remaining activity) (*9*) and eliminates the hydratase activity (*11*). The structural consequences

of this mutation were assessed by determining a crystal structure of the P1A mutant (2.7 Å resolution), and comparing it to that of the wild-type enzyme. The mutant MSAD crystallized with two monomers per asymmetric unit. Least-squares superpositioning using the CCP4 Suite program LSQMAN (*33*) showed that both monomers are virtually identical, aligning with a 0.09 Å rmsd for the C_α atoms. Least-squares superpositioning of the structures of a single wild-type MSAD monomer with the monomers of the mutant yielded a 0.26 Å rmsd for the 129 C_α atoms.

There are no striking differences between the active sites other than the replacement of Pro-1 with an alanine. All other amino acids occupy space similar to that observed for the wild type. Because of the lower resolution, fewer ordered water molecules were included during refinement. However, as in the wild-type structure, ordered water molecules are observed within hydrogen bonding distances of the prolyl nitrogen of Pro-1 (2.9 Å), one of the two η-nitrogens of the side chain guanidinium group of Arg-75 (2.8 Å), and the carboxylate oxygen of Asp-37 (3.0 Å). In view of the structural similarities, the observed decrease in activity for the P1A mutant is likely a direct effect of the substitution of proline with an alanine, which alters both the pK_a and flexibility of the catalytic acid.

*Crystal Structure of MSAD Inactivated by **8***. It has previously been found that **8** is a mechanism-based inhibitor of MSAD (*12*). Mass spectral analysis of MSAD inactivated by **8** showed that the sole site of modification on the protein is Pro-1, and that the increase in molecular mass is consistent with modification by a 3-oxopropanoate moiety. The crystal structure of the inactivated MSAD was determined to 1.6 Å resolution by the molecular replacement method and refined to R and R_{free} values of 19.6 and 24.3%, respectively. Inspection of the σ_A-weighted $2mF_o - DF_c$ electron density map showed the covalent modification of the amino group of Pro-1 with a 3-oxopropanoate moiety (Figure 5). No other residue is modified. These observations fully support the mass spectral analysis and further confirm the location of the active site.

The 3-oxopropanoate moiety forms three additional interactions with active site residues (Figure 5). Asp-37 forms a hydrogen bond with the carbonyl oxygen (2.4 Å) of the 3-oxopropanoate moiety, from which it can be inferred that Asp-37 is an acid. One carboxylate oxygen of the 3-oxopropanoate moiety is within hydrogen bonding distance of the main chain nitrogen of Arg-73 (2.7 Å) and the side chain η-nitrogen of Arg-75 (3.1 Å). The second carboxylate oxygen interacts with the side chain ϵ-nitrogen of Arg-73 (2.9 Å). These observations combined with those made for the active site of the wild type and the results of mutagenesis experiments suggest mechanisms for the inactivation of MSAD by **7** and **8**, the hydration of **5**, and the decarboxylation of **3**.

Mutagenesis of Asp-37 and Arg-73. To investigate the importance of Asp-37 and Arg-73 for the decarboxylase and hydratase activities of MSAD, D37N and R73A mutants were constructed. After DNA sequencing confirmed that only the intended mutation had been introduced, the protein products were overexpressed in *E. coli* BL21(DE3) and purified to homogeneity (as assessed by SDS−PAGE) using the protocol described for wild-type MSAD (*9*). The yields (in milligrams of homogeneous protein per liter of cell culture) were comparable to that of the wild type (typically, ∼20−30 mg/L). Analysis of the purified products by ESI-MS indicated that the subunit had the expected mass, and was not blocked by the initiating formylmethionine. The elution times for the three mutants and the wild-type MSAD are comparable (∼38 min at a flow rate of 0.4 mL/min) during gel filtration chromatography, indicating that the homotrimeric structures of the mutants are intact and that global conformation changes had not occurred as a result of the mutations.

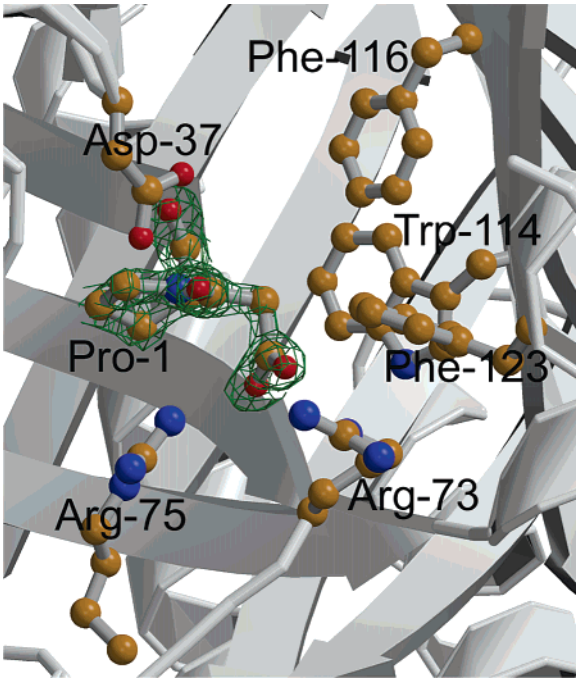

FIGURE 5: σ_A-weighted $2mF_o - DF_c$ electron density for the covalently modified Pro-1 identifying one active site of the inactivated MSAD homotrimer. The electron density of Pro-1 modified by 3-oxopropanoate is colored green. The 3-oxopropanoate moiety is within hydrogen bonding distance of Asp-37, Arg-73, and Arg-75 (see the text). Elements of the hydrophobic wall (Trp-114, Phe-116, and Phe-123) are also shown. This figure was prepared with RASTER3D (*20*) and BOBSCRIPT (*34*).

The decarboxylase and hydratase activities of these two mutants were determined. The purified D37N mutant showed a decarboxylase activity of 250 milliunits/mg of protein, which is only 0.5% of the specific activity observed for the wild-type enzyme (49 000 milliunits/mg). The purified R73A mutant showed a decarboxylase activity of 700 milliunits/mg of protein, which is 1.8% of the specific activity observed for the wild-type enzyme (38 000 milliunits/mg).[4] The hydratase activities for the D37N and R73A mutants were not detectable. The results clearly indicate that Asp-37 and Arg-73 are each critical for both activities.

Mechanism of Inactivation. The crystal structure of the inactivated complex suggests that the carboxylate group of **8** is positioned in the active site by its interaction with the two arginine residues, Arg-73 and Arg-75 (Figure 6, top panel). This binding mode places C-3 and C-2 proximal to Asp-37 and Pro-1. Conceivably, the chloride could interact with the residues comprising the hydrophobic region (e.g.,

[4] Because of the variability in the measurement of the specific activities, mutant activities were determined and compared side by side with wild-type specific activity.

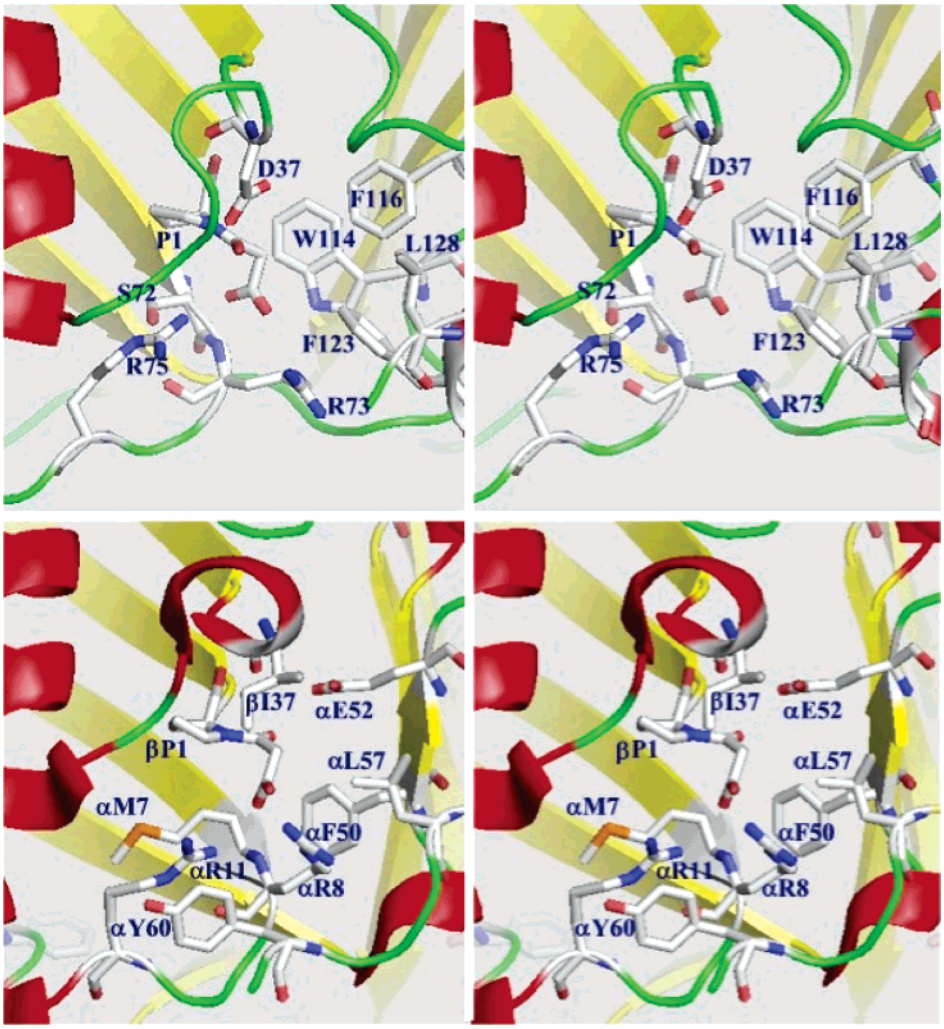

FIGURE 6: Comparison of MSAD (top) and CaaD (bottom) inactivated by 3-oxopropanoate. Pro-1 and the two arginine residues are positionally conserved in the two structures; on the other hand, Asp-37 in MSAD is replaced with *β*Ile-37 in CaaD and Phe-116 in MSAD is replaced with αGlu-52 in CaaD. The orientation of the 3-oxopropanoate moiety is governed by hydrogen bonding between the 3-carbonyl oxygen and Asp-37 (MSAD) or αGlu-52 (CaaD), as described in the text. This figure was prepared with PyMOL (*26*).

Scheme 3

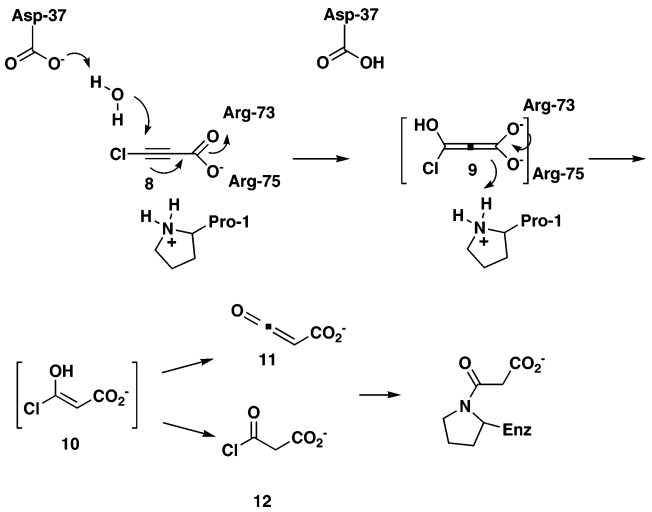

Trp-114, Phe-116, Phe-123, and Leu-128). The presence of a network of water molecules suggests that Asp-37 could abstract a proton from a water molecule for addition to C-3 of **8** (Scheme 3). It is noteworthy that in the inactivated complex, Asp-37 forms a hydrogen bond with the carbonyl oxygen of the 3-oxopropanoate moiety. The hydrogen bonding capability of Asp-37 in this complex suggests that it has abstracted a proton from a water molecule. Interactions between Arg-73 and Arg-75 and the carboxylate group of **8** would polarize the α,*β*-unsaturated acid and favor the formation of a partial positive charge at C-3 (*12*). The allenediolate species (e.g., **9**) can be stabilized by the interaction with the arginine residues. Collapse of **9**, with concomitant protonation at C-2, proposed to be carried out by Pro-1, results in **10**. An enzyme-catalyzed or nonenzymatic rearrangement of **10** produces a ketene (**11**) or an acyl chloride (**12**). Modification of Pro-1 results because the prolyl nitrogen becomes deprotonated (and nucleophilic) in the course of the hydration reaction (*12*).

Mechanism for the Hydration of 5. The enzyme-catalyzed Michael addition of water to **5** requires activation of a water molecule and polarization of the α,*β*-unsaturated carbonyl group of **5**. As proposed above, Asp-37 could activate a water molecule for nucleophilic attack at C-4 of **5** (Scheme 4) to initiate the Michael addition of water. Arg-73 and Arg-75 could polarize the carbonyl oxygen and assist in binding of the carboxylate group. Pro-1 is an obvious candidate to provide a proton at C-3 to complete the Michael addition of water. Ketonization of **13** to **6** could be an enzyme-catalyzed process or result from a nonenzymatic rearrangement.

Scheme 4

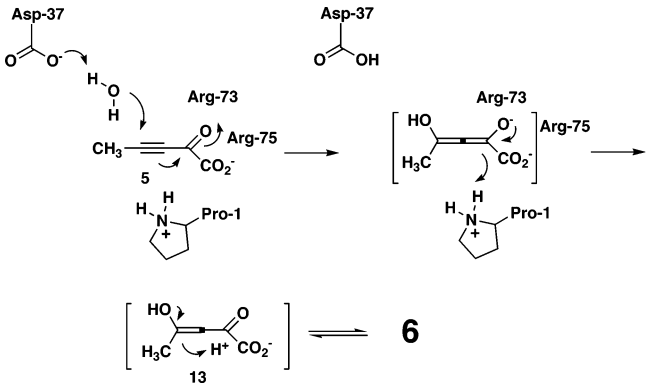

Scheme 5

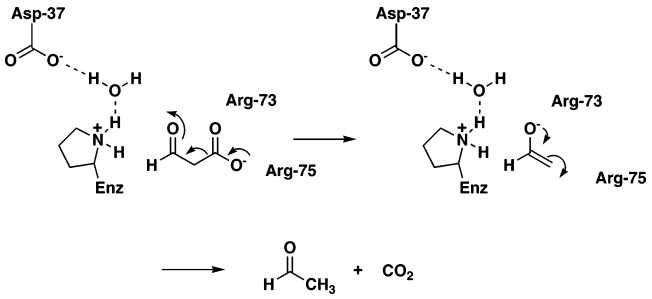

Mechanism of Decarboxylation. Three mechanisms for the decarboxylation of **3** have been proposed and previously examined (*9*, *11*). A metal ion-dependent decarboxylation can be ruled out for three reasons: the addition of various metal ions does not stimulate activity, incubation with EDTA does not diminish activity, and metal ions are not observed in any of the high-resolution crystal structures (*9*). A Schiff base mechanism is also unlikely because the only available base in the active site is Pro-1 and the prolyl nitrogen, with a pK_a of ~9.2, is predominately cationic at cellular pH (*9*, *11*). The crystal structures of wild-type MSAD and MSAD inactivated by **8** also show that the nearest lysine residue, Lys-4, is 12 Å from the active site and, in the absence of a major conformational change upon substrate binding, is not likely to participate in catalysis. For these reasons, the formation of a Schiff base is not favored.

The available evidence supports the third mechanism in which the cationic Pro-1 polarizes the carbonyl group of **3** (Scheme 5). In this mechanism, Asp-37 may play an indirect role in catalysis and be partially responsible for the observed pK_a of Pro-1 (~9.2) (*11*). This putative role for Asp-37 is based on its participation in the hydrogen bond network. A disruption of this network and a decrease in the pK_a for the prolyl nitrogen could account, in part, for the diminished activity of the D37N mutant. Arg-73 and Arg-75 could have dual purposes. First, one or both could assist Pro-1 in stabilizing the developing charge of the enolate anion. Second, one or both arginines could position the carboxylate group of substrate such that the scissile bond (C-1−C-2) is parallel to the p-orbitals of the carbonyl group. This conformation would facilitate decarboxylation. Pro-1 might be responsible for protonation of the resulting enolate anion intermediate.

A somewhat analogous mechanism has been proposed for methylmalonyl-CoA decarboxylase (MMCD), an enzyme found as part of a pathway that converts succinate to propionate in *E. coli* (*7*). On the basis of crystallographic observations, Benning et al. proposed that the backbone amide groups of His-66 and Gly-110 provide two hydrogen bonds to the thioester carbonyl oxygen of methylmalonyl-CoA (*7*). The strategically placed hydrogen bonds form an oxyanion hole that polarizes the carbonyl oxygen bond and stabilizes the anion intermediate. It was further proposed that Tyr-140 orients the carboxylate group of the substrate orthogonal to the plane of the thioester carbonyl group. Finally, the active site cavity is largely hydrophobic (other than Tyr-140), which would enhance the loss of the negatively charged carboxylate group.

*Comparison of the Structures of MSAD Inactivated by **8** and CaaD Inactivated by **7***. Inactivation of MSAD by **8** and CaaD by **7** results in an enzyme modified at the prolyl nitrogen by a 3-oxopropanoate moiety (*12*, *18*, *24*). The corresponding crystal structures show a high degree of structural homology (Figure 6). Superpositioning of the two structures shows a 3.9 Å rmsd for the C_α atoms and a 4.1 Å rmsd for all atoms. The active site residues of MSAD (Pro-1, Leu-2, Asp-37, Arg-73, Arg-75, Trp-114, Phe-116, and Leu-128) (Figure 6, top panel) correspond to mostly similar ones in the CaaD active site (βPro-1, βPhe-2, βIle-37, αArg-8, αArg-11, αPhe-50, αGlu-52, and αLeu-57) (Figure 6, bottom panel). The amino-terminal prolines (Pro-1 and βPro-1) and the arginines (Arg-73 and αArg-8, and Arg-75 and αArg-11) are positionally conserved in the two structures. However, Phe-116 of MSAD occupies the position of αGlu-52 in CaaD, and Asp-37 of MSAD occupies the position of βIle-37 in CaaD. The interchange of these acidic and hydrophobic side chains in the active site impacts the enzymes' interactions with the 3-oxopropanoate moiety and may have implications for the two different reactions catalyzed by the two enzymes (i.e., decarboxylation vs dehalogenation) as well as the efficiencies of the common reaction (e.g., hydration of **5**, **7**, and **8**).

The orientation of the 3-oxopropanoate moiety in both active sites appears to be governed by hydrogen bonding between the 3-carbonyl oxygen and either αGlu-52 (CaaD) or Asp-37 (MSAD). In CaaD, the 3-carbonyl oxygen is within hydrogen bonding distance of a carboxylate oxygen of αGlu-52. In MSAD, the 3-carbonyl oxygen is within hydrogen bonding distance of a carboxylate oxygen of Asp-37. As a result, the carboxylate group of the 3-oxopropanoate moiety interacts differently with the positionally equivalent arginines. In CaaD, a carboxylate oxygen interacts with the backbone nitrogen of αArg-8 (3.0 Å) and the guanidinium group of αArg-11 (2.7 Å). In MSAD, one carboxylate oxygen of the 3-oxopropanoate moiety interacts with the side chain ϵ-nitrogen of Arg-73 (positionally equivalent to αArg-8), and the other carboxylate oxygen interacts with the main chain nitrogen of Arg-73 and the side chain η-nitrogen of Arg-75 (positionally equivalent to αArg-11) (Figure 6). Interestingly, in both structures, an aromatic side chain stacks with the guanidinium side chain of one of the two arginines (Phe-123 with Arg-73 in MSAD and αTyr-60 with αArg-11 in CaaD), thereby orienting the arginine residue. The importance of this subtle difference to the different chemistries of the two enzymes remains to be determined.

The similarities, and subtle differences, between the two active sites are intriguing in view of the very different reactions catalyzed by the two enzymes. The crystal struc-

tures suggest that the different reactions could be due to only a few mutations in the active sites. In MSAD, Phe-116 replaces αGlu-52 and, along with Trp-114, Phe-123, and Leu-128, forms a hydrophobic wall on one side of the active site. The hydrophobic region would destabilize the negatively charged carboxylate group of **3** and favor decarboxylation. It is known that replacing αGlu-52 in CaaD with a glutamine eliminates the dehalogenase activity (*24*). Hence, this mutation (or one in which αGlu-52 is replaced with phenylalanine) coupled with the replacement of *β*Ile-37 with aspartic acid could generate an enzyme with a low-level MSAD activity. These experiments and the analogous ones on MSAD are currently being pursued.

We have previously reported that the consequences of the hydration reactions catalyzed by CaaD and MSAD are the same (i.e., conversion of **5** to **6** and a mechanism-based inactivation by **7** or **8** due to covalent modification of Pro-1), but the overall rates are different (*12*). A comparison of the k_{cat}/K_m values shows that CaaD is ∼10 times more efficient (6400 M^{-1} s^{-1}) than MSAD (600 M^{-1} s^{-1}) in the hydration of **5** to **6**. A very high K_m value for **5** (∼9.6 mM) reduces the catalytic efficiency of MSAD. The 3-halopropiolates are also more efficient inhibitors of CaaD (*18*). For example, CaaD loses ∼80% of its activity in ∼5 s when incubated with a slight excess of **8**. In contrast, the inactivation of MSAD requires higher concentrations (5−50 mM) and longer incubation times (1−7 min) (*12*).

The different rates could be a function of the distance between the water-activating residues, αGlu-52 in CaaD and Asp-37 in MSAD, and Pro-1, coupled with the positioning of **5**, **7**, or **8** due to the interaction between the substrate's carboxylate group and the arginine residues of the enzyme. In the 3-oxopropanoate-modified MSAD structure, Asp-37 and Pro-1 are separated by 3.4 Å, whereas in the 3-oxopropanoate-modified CaaD structure, αGlu-52 and Pro-1 are separated by 4.9 Å.[5] Assuming that the substrate (**5**, **7**, or **8**) binds between the water-activating residue and Pro-1, the additional space in CaaD may make its active site significantly more accommodating. Moreover, the carboxylate groups of these substrates will presumably interact with the two arginine residues, and this interaction may result in unfavorable binding interactions in the active site of MSAD.

Evolutionary Implications. The crystallographic observations reported here along with those reported previously for CaaD (*24*) clearly show structural homology between MSAD and CaaD as well as positional conservation of key catalytic residues (Pro-1 and two arginines) in the active sites. There are also a number of functional similarities between the two enzymes. Both function as hydratases, converting **5** to **6**, and both use an amino-terminal proline (with a pK_a of ∼9.2) and two conserved arginines to catalyze this reaction as well as their physiological reactions (*11*, *18*, *35*). Finally, as a result of the hydration reaction, the 3-halopropiolates are converted to reactive species that alkylate and inactivate both enzymes (*12*, *18*). These similarities and the fact that CaaD and MSAD catalyze successive reactions in the *trans*-1,3-dichloropropene degradation pathway are consistent with the proposal that the two enzymes diverged from an ancestral enzyme that catalyzed both reactions. Hence, the evolutionary route for these two enzymes may provide support for the Horowitz hypotheses about how new enzymes evolve (*36*).

We have previously suggested that an ancestral enzyme may have functioned primarily as a hydratase because the hydration of **2**, an α,*β*-unsaturated acid, is the chemically more difficult reaction (*12*). A random encounter of **3** with the cationic Pro-1 could result in decarboxylation and make this ancestral hydratase an accidental decarboxylase. In the proposed evolutionary scenario, gene duplication gave rise to separate enzymes that retained the components for the hydration reaction along with the rudimentary decarboxylase activity (*37*, *38*).[6] Enhancement of the accidental decarboxylase activity could result from a limited number of mutations (*39*) that increased the probability of encounter and optimized the position of **3** with respect to the cationic Pro-1 and introduced additional catalytic elements to facilitate decarboxylation. A comparison of the crystal structures for MSAD and CaaD suggests a relatively simple route from one tautomerase superfamily activity to a second. For example, two mutations in CaaD (replacing αGlu-52 with phenylalanine and *β*Ile-37 with aspartic acid) might generate an enzyme with MSAD activity. We are currently examining the consequences of these mutations.

[5] These distances are measured from the prolyl nitrogen to a side chain carboxylate oxygen.

[6] It is also noteworthy that CaaD is a heterohexamer consisting of three α,*β*-dimers and MSAD is a homotrimer. The structures could reflect an early duplication event of a small gene, encoding one *β*−α−*β* motif, followed by co-evolution and fusion.

ACKNOWLEDGMENT

Electrospray ionization (ESI) and matrix-assisted laser desorption ionization (MALDI) mass spectrometry were performed by the Analytical Instrumentation Facility Core (College of Pharmacy, The University of Texas), supported by Center Grant ES07784.

SUPPORTING INFORMATION AVAILABLE

Crystallization conditions and experimental procedures used for data collection, heavy atom derivative screening, and structure determinations of MSAD, the MSAD−*p*-chloromercuriphenylsulfonate complex, the P1A mutant, and MSAD inactivated by **8**. This material is available free of charge via the Internet at http://pubs.acs.org.

REFERENCES

1. O'Leary, M. H. (1992) Catalytic Strategies in Enzymic Carboxylation and Decarboxylation, in *The Enzymes*, Vol. 20, pp 235−269, Academic Press, San Diego.
2. Grissom, C. B., and Cleland, W. W. (1986) Carbon isotope effects on the metal ion catalyzed decarboxylation of oxaolacetate, *J. Am. Chem. Soc. 108*, 5582−5583.
3. Hamilton, G. A., and Westheimer, F. H. (1959) On the mechanism of the enzymatic decarboxylation of acetoacetate, *J. Am. Chem. Soc. 81*, 6332−6333.
4. Fridovich, I., and Westheimer, F. H. (1962) On the mechanism of the enzymatic decarboxylation of acetoacetate. II, *J. Am. Chem. Soc. 84*, 3208−3209.
5. Steinberger, R., and Westheimer, F. H. (1951) Metal ion-catalyzed decarboxylation: A model for an enzyme system, *J. Am. Chem. Soc. 73*, 429−435.
6. Seltzer, S., Hamilton, G. A., and Westheimer, F. H. (1959) Isotope effects in the enzymatic decarboxylation of oxalacetic acid, *J. Am. Chem. Soc. 81*, 4018−4024.
7. Benning, M. M., Haller, T., Gerlt, J. A., and Holden, H. M. (2000) New reactions in the crotonase superfamily: Structure of methylmalonyl CoA decarboxylase from *Escherichia coli*, *Biochemistry 39*, 4630−4639.

8. Dunathan, H. C. (1966) Conformation and reaction specificity in pyridoxal phosphate enzymes, *Proc. Natl. Acad. Sci. U.S.A. 55*, 712−716.
9. Poelarends, G. J., Johnson, W. H., Jr., Murzin, A. G., and Whitman, C. P. (2003) Mechanistic characterization of a bacterial malonate semialdehyde decarboxylase: Identification of a new activity in the tautomerase superfamily, *J. Biol. Chem. 278*, 48674−48683.
10. Poelarends, G. J., Wilkens, M., Larkin, M. J., van Elsas, J. D., and Janssen, D. B. (1998) Degradation of 1,3-dichloropropene by *Pseudomonas cichorii* 170, *Appl. Environ. Microbiol. 64*, 2931−2936.
11. Poelarends, G. J., Serrano, H., Johnson, W. H., Jr., Hoffman, D. W., and Whitman, C. P. (2004) The hydratase activity of malonate semialdehyde decarboxylase: Mechanistic and evolutionary implications, *J. Am. Chem. Soc. 126*, 15658−15659.
12. Poelarends, G. J., Serrano, H., Johnson, W. H., Jr., and Whitman, C. P. (2005) Inactivation of malonate semialdehyde decarboxylase by 3-halopropiolates: Evidence for hydratase activity, *Biochemistry 44*, 9375−9381.
13. Andersson, K. (1972) Additions to propiolic and halogen substituted propiolic acids, *Chem. Scr. 2*, 117−120.
14. Sambrook, J., Fritsch, E. F., and Maniatis, T. (1989) *Molecular Cloning*: *A Laboratory Manual*, Cold Spring Harbor Laboratory Press, Plainview, NY.
15. Laemmli, U. K. (1970) Cleavage of structural proteins during the assembly of the head of bacteriophage T4, *Nature 227*, 680−685.
16. Waddell, W. J. (1956) A simple ultraviolet spectrophotometric method for the determination of protein, *J. Lab. Clin. Med. 48*, 311−314.
17. Ho, S. N., Hunt, H. D., Horton, R. M., Pullen, J. K., and Pease, L. R. (1989) Site-directed mutagenesis by overlap extension using the polymerase chain reaction, *Gene 77*, 51−59.
18. Wang, S. C., Person, M. D., Johnson, W. H., Jr., and Whitman, C. P. (2003) Reactions of *trans*-3-chloroacrylic acid dehalogenase with acetylene compounds: Consequences of and evidence for a hydration reaction, *Biochemistry 42*, 8762−8773.
19. Kraulis, P. J. (1991) MOLSCRIPT: A program to produce both detailed and schematic plots of protein structures, *J. Appl. Crystallogr. 24*, 946−950.
20. Merritt, E. A., and Murphy, M. E. (1994) Raster3D Version 2.0. A program for photorealistic molecular graphics, *Acta Crystallogr. D50*, 869−873.
21. Subramanya, H. S., Roper, D. I., Dauter, Z., Dodson, E. J., Davies, G. J., Wilson, K. S., and Wigley, D. B. (1996) Enzymatic ketonization of 2-hydroxymuconate: Specificity and mechanism investigated by the crystal structures of two isomerases, *Biochemistry 35*, 792−802.
22. Taylor, A. B., Johnson, W. H., Jr., Czerwinski, R. M., Li, H.-S., Hackert, M. L., and Whitman, C. P. (1999) Crystal structure of macrophage migration inhibitory factor complexed with (*E*)-2-fluoro-*p*-hydroxycinnamate at 1.8 Å resolution: Implications for enzymatic catalysis and inhibition, *Biochemistry 38*, 7444−7452.
23. Almrud, J. J., Kern, A. D., Wang, S. C., Czerwinski, R. M., Johnson, W. H., Jr., Murzin, A. G., Hackert, M. L., and Whitman, C. P. (2002) The crystal structure of YdcE, a 4-oxalocrotonate tautomerase homologue from *Escherichia coli*, confirms the structural basis for oligomer diversity, *Biochemistry 41*, 12010−12024.
24. de Jong, R. M., Brugman, W., Poelarends, G. J., Whitman, C. P., and Dijkstra, B. W. (2004) The X-ray structure of *trans*-3-chloroacrylic acid dehalogenase reveals a novel hydration mechanism in the tautomerase superfamily, *J. Biol. Chem. 279*, 11546−11552.
25. Nayal, M., Hitz, B. C., and Honig, B. (1999) GRASS: A server for the graphical representation and analysis of structures, *Protein Sci. 8*, 676−679.
26. DeLano, W. L. (2002) *The PyMOL molecular graphics system*, DeLano Scientific, San Carlos, CA.
27. Murzin, A. G. (1996) Structural classification of proteins: New superfamilies, *Curr. Opin. Struct. Biol. 6*, 386−394.
28. Whitman, C. P. (2002) The 4-oxalocrotonate tautomerase family of enzymes: How nature makes new enzymes using a β-α-β structural motif, *Arch. Biochem. Biophys. 402*, 1−13.
29. Poelarends, G. J., Serrano, H., Person, M. D., Johnson, W. H., Jr., Murzin, A. G., and Whitman, C. P. (2004) Cloning, expression, and characterization of a *cis*-3-chloroacrylic acid dehalogenase: Insights into the mechanistic, structural, and evolutionary relationship between isomer-specific 3-chloroacrylic acid dehalogenases, *Biochemistry 43*, 759−772.
30. Sparnins, V. L., Chapman, P. J., and Dagley, S. (1974) Bacterial degradation of 4-hydroxyphenylacetic acid and homoprotocatechuic acid, *J. Bacteriol. 120*, 159−167.
31. Harayama, S., Rekik, M., Ngai, K.-L., and Ornston, L. N. (1989) Physically associated enzymes produce and metabolize 2-hydroxy-2,4-dienoate, a chemically unstable intermediate formed in catechol metabolism via *meta* cleavage in *Pseudomonas putida*, *J. Bacteriol. 171*, 6251−6258.
32. Rosengren, E., Aman, P., Thelin, S., Hansson, C., Ahlfors, S., Bjork, P., Jacobsson, L., and Rorsman, H. (1997) The macrophage migration inhibitory factor MIF is a phenylpyruvate tautomerase, *FEBS Lett. 417*, 85−88.
33. Kleywegt, G. J., and Jones, T. A. (1994). A superposition. CCP4/ESF-EACBM, *Newsletter on Protein Crystallography 31*, 9−14.
34. Esnouf, R. M. (1999) Further additions to MolScript Version 1.4, including reading and contouring of electron-density maps, *Acta Crystallogr. D55*, 938−940.
35. Azurmendi, H. F., Wang, S. C., Massiah, M. A., Poelarends, G. J., Whitman, C. P., and Mildvan, A. S. (2004) The roles of active-site residues in the catalytic mechanism of *trans*-3-chloroacrylic acid dehalogenase: A kinetic, NMR, and mutational analysis, *Biochemistry 43*, 4082−4091.
36. Horowitz, N. H. (1945) On the evolution of biochemical syntheses, *Proc. Natl. Acad. Sci. U.S.A. 31*, 153−157.
37. Jensen, R. A. (1976) Enzyme recruitment in evolution of new function, *Annu. Rev. Microbiol. 30*, 409−425.
38. O'Brien, P. J., and Herschlag, D. (1999) Catalytic promiscuity and the evolution of new enzymatic activities, *Chem. Biol. 6*, R91−R105.
39. Schmidt, D. M. Z., Mundorff, E. C., Dojka, M., Bermudez, E., Ness, J. E., Govindarajan, S., Babbitt, P. C., Minshull, J., and Gerlt, J. A. (2003) Evolution potential of $(\beta/\alpha)_8$-barrels: Functional promiscuity produced by single substitutions in the enolase superfamily, *Biochemistry 42*, 8387−8393.

BI051383M